MITSUBISHI ELECTRIC RESEARCH LABORATORIES
http://www.merl.com

Prediction of Cutting Forces for 5-Axis Ball-End Milling of Free-Form Surfaces

Yaman Boz, Huseyin Erdim, Ismail Lazoglu

TR2010-114 November 2010

Abstract

This paper presents a mechanistic cutting force model for 5-axis ball-end milling cutting force prediction. Cutter/workpiece engagement is determined via newly developed solid modeler based engagement model. Simultaneous 5-axis milling tests are conducted on A17075 workpiece material with a carbide cutting tool for impeller roughing toolpaths for the validation of the proposed model. Validation test demonstrates that presented model is computationally efficient and force predictions are in good agreement with the measured data. The result of validation test is also presented in the paper.

4th CIRP International Conference on High Performance Cutting

Prediction of Cutting Forces for 5-Axis Ball-End Milling of Free-Form Surfaces

Yaman BOZ[1], Huseyin ERDIM[2], and Ismail LAZOGLU[1*]
[1] Manufacturing and Automation Research Center, Koc University, Turkey
[2] Mitsubishi Electric Research Laboratories, USA
[1*] Manufacturing and Automation and Research Center, Koc University, Turkey, ilazoglu@ku.edu.tr

Abstract:
This paper presents a mechanistic cutting force model for 5-axis ball-end milling cutting force prediction. Cutter/workpiece engagement is determined via newly developed solid modeler based engagement model. Simultaneous 5-axis milling tests are conducted on Al7075 workpiece material with a carbide cutting tool for impeller roughing toolpaths for the validation of the proposed model. Validation test demonstrates that presented model is computationally efficient and force predictions are in good agreement with the measured data. The result of validation test is also presented in the paper.

Keywords: 5-axis machining, Milling force model, Sculptured surface machining, Boundary Representation

1. Introduction

5-axis machining technologies have been used in the production of various parts in aerospace, automotive and biomedical industries. With 5-axis machining, complex shapes can be machined in a single setup which reduces cycle times. Improved tool accessibility allows the use of shorter tools that provide more accurate machining. The main aims of using 5-axis machining in industry are to reduce cycle times, dimensional and surface errors in its nature. However, this cannot be achieved satisfactorily without the physical modeling of the milling process. Furthermore, while machining free-form surfaces local peak forces may occur due to spatially changing engagement between the cutter and the workpiece. Hence, cutting force modeling gains more importance in order to prevent excessive cutter deflection and surface errors in these processes.

Most of the research on 5- axis machining focused on the geometric aspects of this process such as toolpath generation, toolpath optimization and geometric verification of the toolpath. With the improvement in the CAM technology geometric constraints and errors can be eliminated, on the other hand, the physics of the process is not considered. Consequently, efficiency of the process and errors due to physical constraints cannot be predicted before the production of the part.

In the modeling of 5-axis machining processes noteworthy research was conducted by Zhu et al. [1] where Z-map technique was utilized for cutter-workpiece engagement for cutting force prediction, then a process fault detection and fault diagnosis methodology was developed. Similarly, Fussell et al. [2] developed a 5-axis virtual machining environment for discrete simulation of sculptured surface machining which aims automatic feedrate selection along the toolpath via mechanistic modeling of cutting forces. Bailey et al. [3, 4] proposed a generic mechanistic cutting force model for simulating multi axis machining of sculptured surfaces. A process optimization tool was presented by employing a feedrate scheduling method using the maximum chip load and cutting force as constraints. Becze et al. [5] introduced an analytical chip load model for 5-axis high-speed milling of hardened tool steel. The effect of tilt angle on cutting forces, tool wear mechanisms and also surface integrity were investigated in this study.

Some of the most recent studies on modeling of 5- axis milling were carried out by Ozturk and Budak [6], Tunc and Budak [7]. Analytical modeling of cut geometry of 5-axis machining was performed and obtained data was used for cutting force prediction and process optimization. Ferry and Altintas [8] developed a virtual machining simulation system for 5-axis flank milling of jet engine impellers.

This article extends the mechanistic modeling of 3-axis ball-end milling presented by Erdim et al. [9, 10] into mechanistic modeling of 5-axis ball-end milling. Boundary representation (B-rep) based exact Boolean method is preferred for extracting cutter/workpiece engagement due to its efficiency and speed over other discrete methods. The model can easily handle complex engagements between tool and workpiece. Comprehensive formulation of cutting force model is given and its validation is demonstrated.

2. Solid Modeler Based Cutter/Workpiece Engagement

In sculptured surface machining, the cutter/workpiece engagement region does vary along the cutter path. In general, it is difficult to find an exact representation of the engagement region for complex surfaces, however there are some specific solutions for simple tool motions and surfaces. Chip load and force calculations are based on the cutter/workpiece engagements; therefore the output of the engagement model is very critical. Mathematically, the swept volume is the set of all points in space encompassed within the object envelope during its motion. The basic idea in NC verification and simulation is to remove the cutter swept volume from the workpiece stock and thus to obtain the final machined surfaces.

In literature, NC machining simulation can be mainly categorized into three major approaches. The first approach is the exact Boolean, the second approach is the spatial partitioning, and the third approach is the discrete vectors. The direct Boolean subtraction approach is an exact and analytical approach. It directly performs the Boolean subtraction operation between a solid model and the volume swept by a cutter between two adjacent tool positions. Although this approach can provide accurate verification and error assessment, the computation cost is known to grow too much for a large number of tool-paths. The second approach uses spatial partitioning representation to define a cutter and the workpiece. In this approach, a solid object is decomposed into a collection of basic geometric elements, for example Z-map (Z-buffer), voxel, and ray representation, thus simplifying the processes of regularized Boolean set operations. However, its computation time and memory consumption are increased drastically to get better accuracy. One of the other widely used NC simulation methods is based on the vector-clipping approach.

In this work, B-rep based method is developed to find the cutter/workpiece engagement (CWE). The most common schemes used in solid modelers are the boundary representation (B-rep) and Constructive Solid Geometry (CSG). In B-rep methodology an object is represented by both its boundaries defined by faces, edges, vertices and the connectivity information. The prototype program is implemented using the commercial Parasolid solid modeler kernel.

In this paper, a validation test is demonstrated for the simulation of impeller 5-axis machining by variable lead and tilt angles. Figure 1 shows the CAD model of impeller part file together with the stock workpiece.

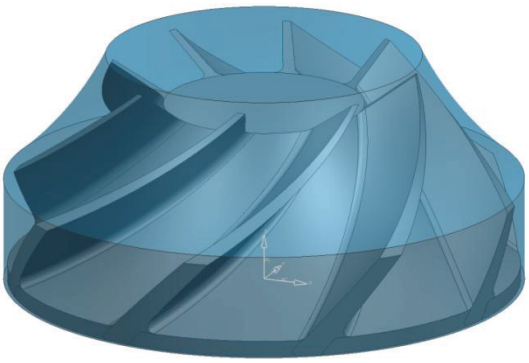

Figure 1: The CAD model of the impeller blade and the stock workpiece

The tool movements are subtracted from the workpiece model by using corresponding Parasolid functions in order to find the in-process machined surface. Figure 2 shows the resultant machined surfaces for the all whole cutter location (CL) points (4374 CL points) for rough machining.

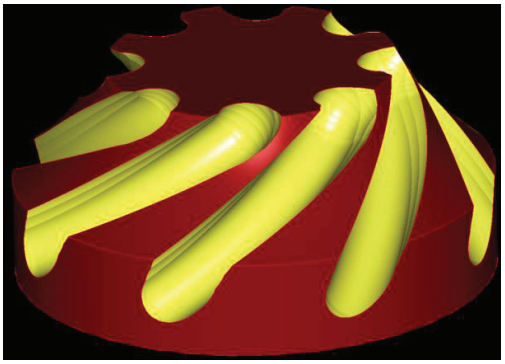

Figure 2: The simulated machined surface of impeller blade for 5-axis rough machining.

Once the in-process workpiece is obtained for each CL point, the contact patch surface between the tool and workpiece can be extracted by using Parasolid functions. Then, the resulting 3D contact surface, as illustrated in Fig. 3, is projected to the plane perpendicular to the cutter axis. This step finds the enclosing boundaries and curves of the contact patch. Since the force model discretizes the cutter into slices perpendicular to the tool axis and to perform force calculation for each slice, the discs at each level are projected to the plane perpendicular to the cutter axis. The discs are shown by circles in view AA in Fig. 3.

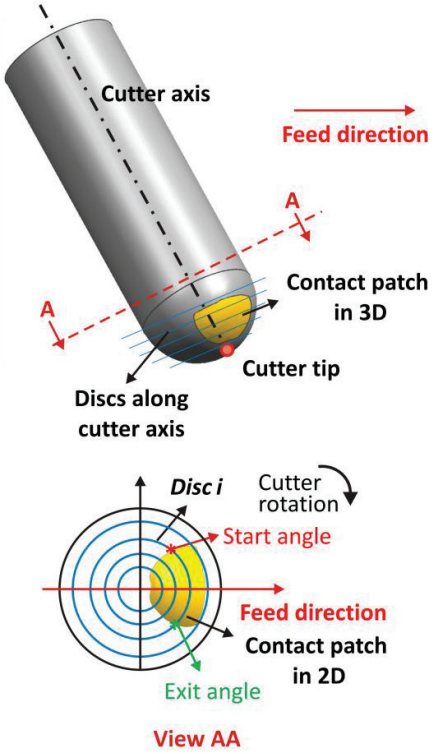

Figure 3: Cutter engagement geometry for ball-end mill

Since engagement domain is simply the combination of start and exit angles of each discrete disc located on the cutter, the next step is to assign the start and exit angles to each respective projected disc by intersecting the 2D discs with the boundaries of the contact patch in plane.

The procedure described above is implemented in Visual Studio.NET using the Parasolid solid modeling

Kernel and Parasolid Workshop on a Windows Core2Duo, 1.8 GHz/4GB Personal Laptop. The forces are compared for one pass where the tool moves from the lower rim of the cylinder workpiece to the upper rim of the cylindrical workpiece. This one pass has 119 CL points, the lead and tilt angles for one-pass is shown together with the simulated workpiece in Fig. 4. The computation time for the engagement domain for this one-pass is 58 seconds for 119 CL points.

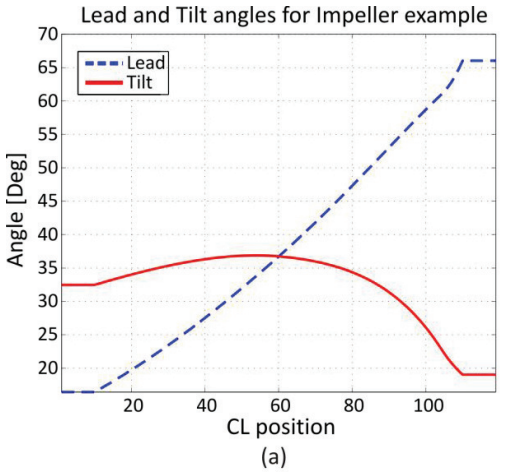

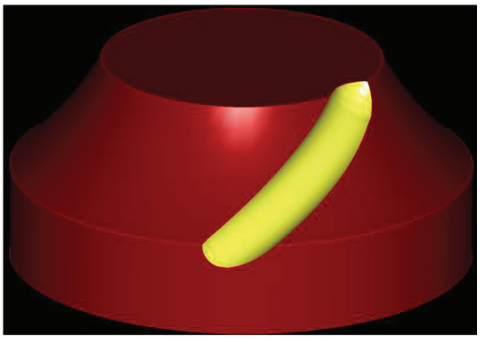

(b)

Figure 4: (a) The lead and tilt angles for one-pass of impeller example, (b) The simulated workpiece for one-pass from Parasolid

The output of the program is processed and the engagement angles are shown together with the contact patches for CL points #20 and #86. Figure 5 shows the engagement domain for CL point #20, where the engagement domain is one piece.

However, the engagement domain can have more than one piece because of the complexity of the geometry of the workpiece and the tool motion as shown simply in Figure 6. In this case, the engagement domain will have more than two intersections for the discs along the cutter.

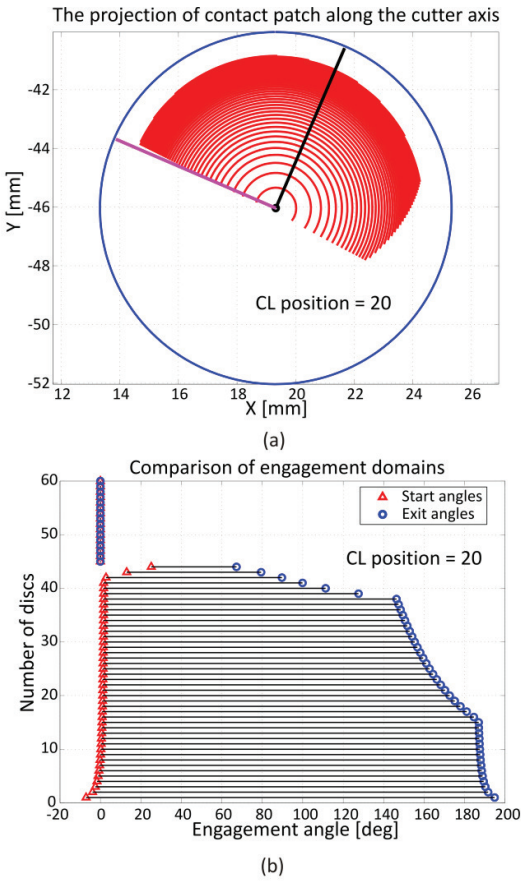

Figure 5: The engagement domain for CL point #20: (a) Projected view of contact patch along cutter axis, (b) Start and exit angles for the discs along the cutter axis.

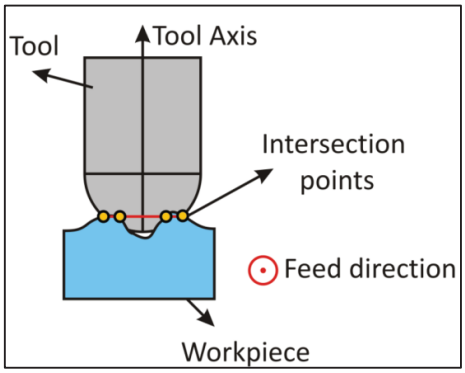

Figure 6: Illustration of multiple contact regions and intersections

There are many tool instances where the engagement domain has more than two pieces for this impeller surface example. The engagement domain for CL point #86 is shown in Figure 7.

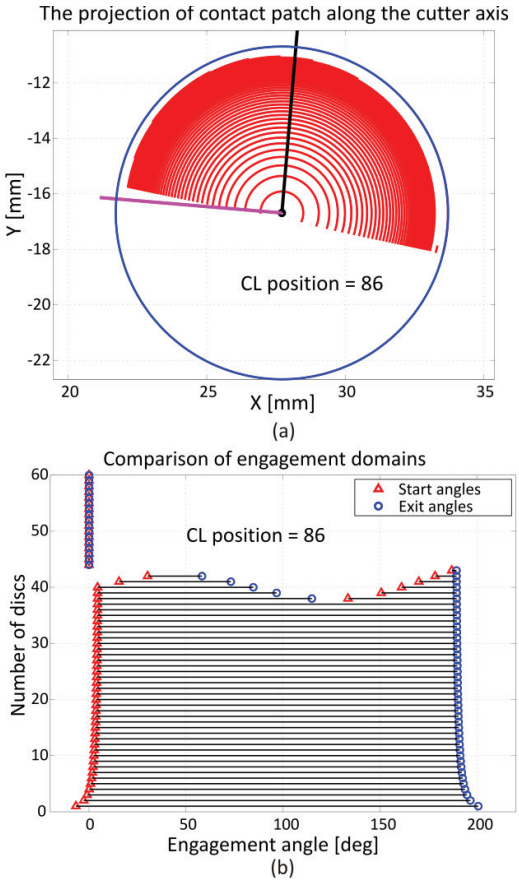

Figure 7: The engagement domain for CL point #86: (a) Projected view of contact patch along cutter axis, (b) Start and exit angles for the discs along the cutter axis.

3. Cutting Force Prediction

5-axis milling geometry differs from 3-axis milling geometry. Hence, transformation from 3-axis milling to 5-axis milling is needed. Necessary transformation is introduced via three coordinate frames shown in Fig 8. Here, $X_w - Y_w - Z_w$ is workpiece coordinate frame (WCF) attached to the workpiece, $X_{TCF} - Y_{TCF} - Z_{TCF}$ is the tool coordinate frame (TCF), and $X_f - Y_f - Z_f$ is the feed coordinate frame.

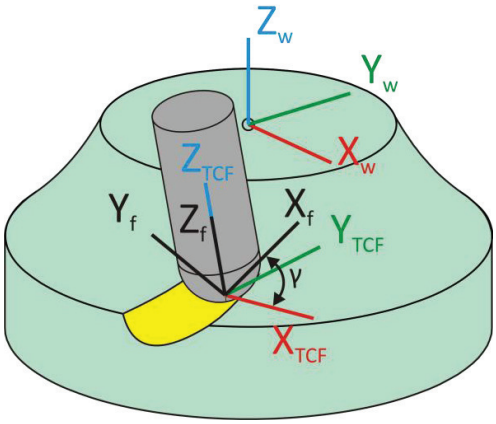

Figure 8: Definition of coordinate frames.

Transformation from feed coordinate frame into TCF is given by

$$B = \begin{matrix} \cos\gamma & -\sin\gamma & 0 \\ \sin\gamma & \cos\gamma & 0 \\ 0 & 0 & 1 \end{matrix} \quad (1)$$

where γ is the angle between feed vector and the X_{TCF}. Final transformation maps the TCF onto WCF as [5]

$$T = \begin{matrix} \cos(l) & \sin\ t\ \sin(l) & -\cos(\mathrm{t})\sin(l) \\ 0 & \cos(t) & \sin\ t \\ \sin(l) & -\sin\ t\ \cos(l) & \cos\ t\ \cos(l) \end{matrix} \quad (2)$$

where l is the lead angle and t is the tilt angle measured relative to Z_{WCF} about Y_{WCF} and X_{WCF} respectively.

In milling, cutting forces depend on instantaneous chip thickness; the uncut chip thickness should be calculated precisely to improve the accuracy of force model that is used in force prediction. In free-form surface machining the distance and the rotation angle between two CL points are relatively small, therefore the effect of rotational velocities of the tool is negligible. For ball-end mill tool, instantaneous undeformed chip thickness is obtained as follows [10];

$$t_{c\ k} =$$

$$t_x \times \sin\ \theta\ \times \sin\ \psi\ \times \cos\ \alpha\ \pm\ t_x \times \cos\ \psi\ \times \sin\ \alpha \quad (3)$$

where $t_{c\ k}$ is the chip thickness, t_x is the feed per tooth, θ is the immersion angle of the cutting point, ψ is the cutting element position angle, and α is the feed inclination angle measured with respect to horizontal feed direction. The immersion angle of a discrete cutting point on the flute of the cutter is given as:

$$\theta = \Omega + 2\pi\ n - 1\quad N_f - \beta_k \quad (4)$$

where θ is the immersion angle for flute n, k represents the number of discrete point on a cutting edge, Ω is the cutting edge rotation angle, N_f is the total number of flutes and β_k is the lag angle due to helix angle of the cutter in the respective k[th] disk.

The instantaneous infinitesimal chip load is written as follows:

$$dA_c = t_{c\ k} \times dz_{\ k} \quad (5)$$

For a differential chip load dA_c in the engagement domain, the differential cutting forces in radial, axial, and tangential directions (r, ψ, t) is written as follows;

$$\begin{aligned} dF_r &= K_{rc} \times dA_c + K_{re} \times dz \\ dF_\psi &= K_{\psi c} \times dA_c + K_{\psi e} \times dz \\ dF_t &= K_{tc} \times dA_c + K_{te} \times dz \end{aligned} \quad (6)$$

where K_{rc}, $K_{\psi c}$ and K_{tc} are radial, axial and tangential cutting force coefficients and K_{re}, $K_{\psi e}$ and K_{te} are cutting edge coefficients respectively. Cutting force and edge coefficients are determined by mechanistic calibration procedure where these coefficients vary along tool axis direction [10].

Transformation matrix A transforms the cutting forces into feed coordinate frame which is initially coincident with TCF. If the angle between feed direction and X_{TCF} is not zero, B matrix transforms the cutting forces into tool coordinate frame.

$$A = \begin{matrix} -\sin\psi \times \sin\theta & -\cos\psi \times \sin\theta & -\cos\theta \\ \sin\psi \times \cos\theta & \cos\psi \cos\theta & -\sin\theta \\ \cos\psi & -\sin\psi & 0 \end{matrix} \quad (7)$$

In this study, a table type dynamometer is used. Therefore, cutting forces in feed coordinate frame are transformed into WCF which is also dynamometer coordinate frame. By using transformation matrix T given in Eq. 2, cutting forces in WCF is written as:

$$\begin{matrix} dF_X \\ dF_Y \\ dF_Z \end{matrix} = T\ B\ A \times \begin{matrix} dF_r \\ dF_\psi \\ dF_t \end{matrix} \quad (8)$$

4. Simulation and Experimental Results

An impeller roughing toolpath is simulated for the cutting force prediction of 5-axis ball-end milling. As it is demonstrated in Fig. 4 (a) lead angles vary between 17° and 66°, and tilt angles vary between 32° and 19°. The simulated toolpath is shown in Figure 9. Dimensions of the blank workpiece and the workpiece coordinate frame are also illustrated in Fig. 9.

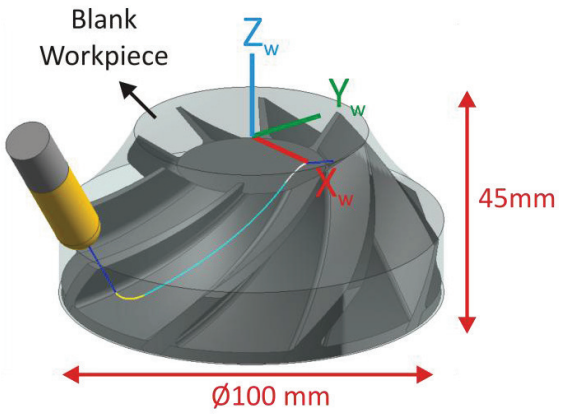

Figure 9: Simulated impeller roughing toolpath

Kistler 9257B type dynamometer is used for measuring forces which is attached to the rotary table of the Mori Seiki NMV5000 DCG machine. The spindle speed and the feedrate for these toolpaths are kept constant at 600 rpm and 48 mm/min respectively. Sandvik two fluted ball-end mill with a diameter of 12 mm, nominal helix angle of 30°, and projection length of 37 mm is used as the cutting tool and Al7075 as workpiece material. Depths of cuts during the toolpath vary approximately between 0 – 5 mm along tool axis.

Figure 10 shows the comparison of the resultant cutting forces for simulated and measured cases. As it is demonstrated in the Fig. 10 simulated and experimental cutting forces match quite well not only in their trends but also in their amplitudes. In most of the regions, the error between simulation and the experimental force amplitudes is below 20 % which can be considered as acceptable for simultaneous 5-axis milling process simulations.

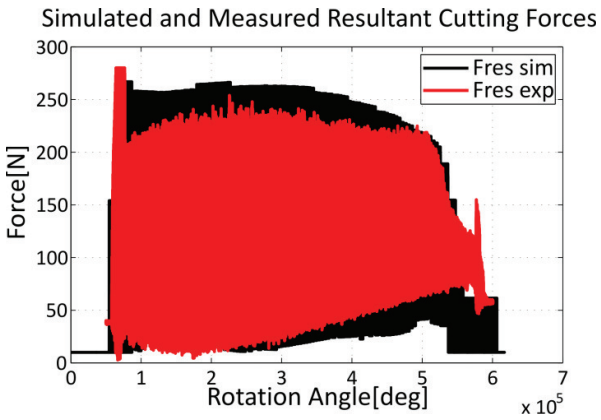

Figure 10: Impeller toolpath simulation and experimental resultant cutting force comparison

The main differences in cutting force predictions can be attributed to use of a table top dynamometer for this test. While machining the workpiece on the machine tool the workpiece has a contribution on the cutting forces due to its weight, furthermore this force component is not constant and change relative to rotation of the rotary axes of the machine tool. Experimental setup of impeller machining test is shown in Fig. 11.

Figure 11: Experimental Impeller machining test

Another reason for the discrepancy in the cutting forces is due to induced cutting force component by the cutting torque. Workpiece length is adjusted to be approximately 150 mm in order to avoid the risk of collisions; therefore this induces the forces due to cutting torque. Hence, more accurate validation of the proposed approach may be performed by using a rotary dynamometer as a future work.

5. Conclusion

In this paper, Solid model based, Boundary Representation engagement model and a physical model for the prediction of cutting forces in 5-axis ball-end milling process are presented. The approach developed based in this model is modular. Therefore, different cutter

and workpiece geometries and tool motions can be incorporated into the model without additional analysis. The model has the ability to calculate complex workpiece/cutter intersection domain automatically for a given CL file, cutter and free-form workpiece geometry.

The presented model can be used in industry, for process simulation and process optimization and it can be integrated into CAD/CAM programs. Cutting parameters of an existing 5-axis ball-end milling process can be used in the model to simulate the cutting forces and optimize the feedrate and other cutting parameters in the process.

Acknowledgement

The authors acknowledge the Machine Tool Technologies Research Foundation (MTTRF), the Mori Seiki Co., and the DP Technology Corp for the Mori Seiki NMV 5000DCG CNC Machining Center and Esprit CAM software supports. The authors also acknowledge Sandvik Coromant Company for providing cutting tools for this research.

References

[1] Zhu, R., Kapoor, S. G., and DeVor, R. E., 2001, Mechanistic Modeling of the Ball End Milling Process for Multi-Axis Machining of Free-Form Surfaces, ASME Journal of Manufacturing Science and Engineering, Vol.123, No. 3, pp. 369–379.

[2] Fussell, B. K., Jerard, R. B., Hemmett, J. G., 2003, Modeling of Cutting Geometry and Forces for 5-Axis Sculptured Surface Machining, Computer-Aided Design, Vol. 35, No.4, pp. 333–346.

[3] Bailey, T., Elbestawi, M. A., El-Wardany, T. I., Fitzpatrick, P., 2002, Generic Simulation Approach for Five-Axis Machining, Part I: Modeling Methodology, ASME Journal of Manufacturing Science and Engineering, Vol. 124, No.3, pp. 624–633.

[4] Bailey, T., Elbestawi, M. A., El-Wardany, T. I., Fitzpatrick, P., 2002, Generic Simulation Approach for Five-Axis Machining, Part II: Model Calibration and Feed Rate Scheduling, ASME Journal of Manufacturing Science and Engineering, Vol. 124, No.3, pp. 634–642.

[5] Becze, C. E., Clayton, P., Chen, L., El-Wardany, T. I., Elbestawi, M. A., 2000, High-Speed Five-Axis Milling of Hardened Tool Steel, International Journal of Machine Tools and Manufacture, Vol. 40, No.6, pp. 869–885.

[6] Ozturk, E., Budak, E., 2007, Modeling of 5-Axis Milling Processes, Machining Science and Technology, Vol. 11, No.3, pp. 287-311.

[7] Tunc L.T., Budak, E., 2009, Extraction of 5-axis milling conditions from CAM data for process simulation, International Journal of Advanced Manufacturing Technology, Vol. 43, No.5-6, pp. 538-550.

[8] Ferry W. B., Altintas Y., 2008, Virtual Five-Axis Flank Milling of Jet Engine Impellers-Part I: Mechanics of Five-Axis Flank Milling, Transactions of ASME Journal of Manufacturing Science and Engineering, Vol. 130, No.1, pp. 51-61.

[9] Erdim H., Lazoglu I., Ozturk B., 2006, Feedrate Scheduling Strategies for Free-Form Surfaces, International Journal of Machine Tools and Manufacture, Vol. 46, No. 7-8, pp. 747–757.

[10] Erdim H., Lazoglu I., Kaymakci M., 2007, Free-Form Surface Machining and Comparing Feedrate Scheduling Strategies Machining Science and Technology, Vol. 11, No. 1, pp. 117-133.